IEEE Access
Multidisciplinary | Rapid Review | Open Access Journal

Received July 19, 2020, accepted July 25, 2020, date of publication July 30, 2020, date of current version August 13, 2020.

Digital Object Identifier 10.1109/ACCESS.2020.3013151

Interval Probabilistic Energy Flow Calculation of CCHP Campus Microgrid Considering Interval Uncertainties of Distribution Parameters

YUQUAN XIE, SHUNJIANG LIN, (Member, IEEE), WEIKUN LIANG, YUERONG YANG, ZHIQIANG TANG, YUNONG SONG, AND MINGBO LIU, (Member, IEEE)
School of Electric Power Engineering, South China University of Technology, Guangzhou 510640, China

Corresponding author: Shunjiang Lin (linshj@scut.edu.cn)

This work was supported in part by the National Natural Science Foundation of China under Grant 51977080, and in part by the Fundamental Research Funds for the Central Universities of China under Grant 2019MS015.

ABSTRACT Due to the absence of historical data and the errors of measurement instruments, there may be uncertainties in the distribution parameters of the random variables describing the uncertain fluctuations of node power including renewable energy station output and load power in the combined cooling heating and power (CCHP) campus microgrid. In this paper, intervals are used to describe the uncertainties of distribution parameters of the random variables, and an interval probabilistic energy flow (IPEF) calculation model of the CCHP campus microgrid is established. Introducing the interval arithmetic (IA) into the cumulant method, an IA-based IPEF algorithm is proposed to obtain the analytical expressions of probability density function or cumulative distribution function intervals of the state variables. Moreover, affine arithmetic (AA) is introduced to address the interval extension problem in the calculation, and an AA&IA-based IPEF algorithm is proposed. By constructing the correlation transformation matrixes, the correlation among different node power is considered in the IPEF calculation. A case study on a CCHP campus microgrid demonstrates that the results of the AA&IA-based IPEF algorithm are more accurate than those of the IA-based IPEF algorithm by using the results of the double-layer Monte Carlo method as a reference. Moreover, the proposed algorithms are more efficient than the double-layer Monte Carlo method.

INDEX TERMS CCHP campus micro-grid, interval probabilistic energy flow calculation, higher-order uncertainty, cumulant method, interval arithmetic, affine arithmetic, correlation.

NOMENCLATURE

A. ACRONYMS

AA	Affine arithmetic
CCHP	Combined cooling heating and power
CDF	Cumulative distribution function
CI	Cumulant interval
CCHP-CMG	CCHP campus micro-grid
DMC	Double-layer Monte Carlo
IA	Interval arithmetic
IPEF	Interval probabilistic energy flow
PDF	Probability density function
PEF	Probabilistic energy flow
PPF	Probabilistic power flow
PT	Photothermic
PV	Photovoltaic

B. PARAMETERS

c_w	Specific heat capacity of water
s	Mark of heating/cooling network, 1/−1 respectively represent heating/cooling network
D	Pipeline resistance coefficient
G_{ij}, B_{ij}	Real and imaginary parts of the i-th row and j-th column element of node admittance matrix
C_m	Heat-to-power ratio
Z	Ratio of thermal and electrical power change of extraction condensing unit
P_{CON}	Electrical power generation of the extraction condensing unit in full condensing mode

The associate editor coordinating the review of this manuscript and approving it for publication was Zhiyi Li.

This work is licensed under a Creative Commons Attribution 4.0 License. For more information, see https://creativecommons.org/licenses/by/4.0/

η_{E}	Conversion efficiency of multi-energy coupling elements
$A_{\mathrm{PV}}/A_{\mathrm{PT}}$	Area of PV panel and PT panels
$\eta_{\mathrm{PV}}/\eta_{\mathrm{PT}}$	Conversion efficiency of PV/PT stations
$r_{\max}$	Maximum of solar irradiance in a period
θ_{PV}	Power factor angle of PV station
$\mu_{\mathrm{L}}/\sigma_{\mathrm{L}}^2$	Mean and variance of load power
$\underline{\mu}_{\mathrm{L}}/\bar{\mu}_{\mathrm{L}}$	Upper and lower bounds of interval $[\mu_{\mathrm{L}}]$
$\underline{\sigma}_{\mathrm{L}}^2/\bar{\sigma}_{\mathrm{L}}^2$	Upper and lower bounds of interval $[\sigma_{\mathrm{L}}^2]$
$\mu_{\mathrm{PV}}/\mu_{\mathrm{PT}}$	Means of power output of PV/PT stations
α, β	Shape parameters of β-distribution

C. VARIABLES

$\boldsymbol{m}_{\mathrm{h/c}}$	Flow rates of the heating/cooling pipe
$\boldsymbol{T}_{\mathrm{s.h/c}}$	Supply temperature at nodes
$\boldsymbol{T}_{\mathrm{r.h/c}}$	Return temperature at nodes
$\boldsymbol{\Phi}_{\mathrm{h/c}}$	Heating/cooling power
$\boldsymbol{\Phi}_{\mathrm{L.h/c}}$	Heating/cooling load power
$\boldsymbol{\Phi}_{\mathrm{PT}}$	Heating power output of the PT stations
$\boldsymbol{m}_{\mathrm{q.h/c}}$	Flow rates at nodes
$\boldsymbol{B}_{\mathrm{h/c}}$	Loop-pipe correlation matrix
$\boldsymbol{A}_{\mathrm{s.h/c}}$	Matrix related to the supply network structure and flow rates
$\boldsymbol{A}_{\mathrm{r.h/c}}$	Matrix related to the return network structure and flow rates
$\boldsymbol{b}_{\mathrm{s.h/c}}$	Vector related to the supply network structure and the supply water temperature at the source node
$\boldsymbol{b}_{\mathrm{r.h/c}}$	Vector related to the return network structure and the return water temperature at the load node
P_i, Q_i	Injected active and reactive power at i-bus of the power network
$P_{\mathrm{L}i}$, $Q_{\mathrm{L}i}$	Active and reactive power of load at i-bus of the power network
$P_{\mathrm{PV}i}$, $Q_{\mathrm{PV}i}$	Active and reactive power of PV stations at i-bus of the power network
U_i	Voltage magnitude at i-bus
δ_{ij}	Voltage phase angle difference between i-bus and j-bus.
Φ_{CCHP}, P_{CCHP}	Total wasted heat power and electrical power of CCHP unit
Φ_{in}, Φ_{out}	Input/output power of energy conversion components
$\boldsymbol{W}$	Injected power vector at buses or nodes
$\boldsymbol{X}$	State variable vector
$\boldsymbol{F}$	Augmented vector of injected power
$\boldsymbol{W}_0$, $\boldsymbol{X}_0$, $\boldsymbol{F}_0$	Reference value of $\boldsymbol{W}/\boldsymbol{X}/\boldsymbol{F}$
$\Delta\boldsymbol{W}$, $\Delta\boldsymbol{X}$, $\Delta\boldsymbol{F}$	Random fluctuation of $\boldsymbol{W}/\boldsymbol{X}/\boldsymbol{F}$
$\boldsymbol{S}_0$	Sensitivity matrix
$\gamma_{\Delta\mathrm{X}}^{(k)}$, $\gamma_{\Delta\mathrm{W}}^{(k)}$	k-order cumulants vectors of $\Delta\boldsymbol{X}$ and $\Delta\boldsymbol{W}$
$[\gamma_{\Delta\mathrm{X}}^{(k)}]$,$[\gamma_{\Delta\mathrm{W}}^{(k)}]$	k-order CI vector of $\Delta\boldsymbol{X}$ and $\Delta\boldsymbol{W}$
$[\gamma_{\mathrm{L\_e/h/c}}^{(k)}]$	k-order CI vector of load power
$[\gamma_{\Delta\mathrm{L.e/h/c}}^{(k)}]$	k-order CI of load power fluctuation
$[M_{\mathrm{r}}^{(k)}]$	k-order origin moment interval of r
$[\gamma_{\mathrm{r}}^{(k)}]$	k-order CI of r
$[\gamma_{\mathrm{PPV}}^{(k)}]$, $[\gamma_{\mathrm{QPV}}^{(k)}]$	k-order CI of active/reactive power of PV station
$[\gamma_{\mathrm{PV}}^{(k)}]$, $[\gamma_{\mathrm{PT}}^{(k)}]$	k-order CI of injected power of PV/PT station
$[\gamma_{\Delta\mathrm{PV}}^{(k)}]$, $[\gamma_{\Delta\mathrm{PT}}^{(k)}]$	k-order CI of PV/PT power fluctuation
$\Delta\boldsymbol{F}_{\mathrm{L}}$, $\Delta\boldsymbol{F}_{\mathrm{S}}$	Random fluctuations of node power augmented vectors of loads and renewable energy stations considering the correlation.
$\Delta\boldsymbol{F}'_{\mathrm{L}}$, $\Delta\boldsymbol{F}'_{\mathrm{S}}$	Decorrelated random fluctuations of node power augmented vectors of loads and renewable energy stations
$\boldsymbol{K}_{\mathrm{L}}$, $\boldsymbol{K}_{\mathrm{S}}$	Correlation conversion matrixes corresponding to the node power of loads and renewable energy stations

D. SUBSCRIPTS AND SUPERSCRIPTS

$(\cdot)^{<k>}$	Calculate the kth power of each element in the matrix
$(\cdot)_{\mathrm{e/h/c}}$	Variables of electricity/heating/cooling network

I. INTRODUCTION

CCHP technology can fully recycle the wasted heat of gas-fired power generators for cooling and heating, which can effectively increase the utilization rate and realize the cascade utilization of energy. Thus, in recent years, CCHP technology has been widely applied in emerging industrial campuses, and many CCHP campus microgrid (CCHP-CMG) projects have been established [1], [2]. The probability density functions of random variables are usually used to describe the uncertain fluctuation characteristics of the electrical/heating/cooling load power and the power output of photovoltaic (PV) / photothermic (PT) stations in the CCHP-CMG, and the uncertain fluctuation characteristics of its operating state can be obtained by probabilistic energy flow (PEF) calculation [3], [4]. However, due to factors such as the absence of historical data and the errors of measurement instruments, there may be uncertainty in the distribution parameters of the PDFs of the random variables describing the uncertain node power in the CCHP-CMG. This uncertainty can be classified as higher-order uncertainty [5], [6]. In addition, the power output of different renewable energy stations and the different types of load power in a CCHP-CMG always have obvious correlation. Therefore, it is of great significance to study the PEF calculation method of a CCHP-CMG considering the higher-order uncertainty and the correlation of node power including renewable energy station output and load power.

Many research articles have been published on the topic of probabilistic power flow (PPF) / probabilistic energy

flow (PEF) calculation in power systems or integrated energy systems. In the PPF calculation of power systems, the following methods are mainly used: simulation method, approximation method, and analytical method [7]. Among them, the analytical method can simultaneously meet the requirements of calculation accuracy and efficiency and obtain the analytical expressions of the probability density function (PDF) or cumulative distribution function (CDF) of state variables, which has received the most attention. In some studies, the analytical solution of the PPF calculation was obtained by convolution computation, but the calculation process was complicated [8]–[10]. The cumulant method can avoid the convolution computation of random variables and improve the calculation efficiency. For example, Zhang and Lee [11] and Fan *et al.* [12] applied the cumulant method and Gram-Charlier expansion to solve the PPF calculation problem. Cai *et al.* [13] used Cholesky decomposition to deal with the correlation of random variables in the cumulant method. For the PEF calculation of integrated energy systems, the cumulant method was applied to the PEF calculation of an electric-gas energy system in [3]. Khorsand and Seifi [4] studied the probability characteristics of load power and failure and solved the PEF calculation of electricity/gas/heating network based on the point estimation method. Chen *et al.* [14] and Yang *et al.* [15] considered the uncertainty of distributed generation and pipeline parameters, respectively, and proposed methods to solve the PEF calculation problem based on Latin hypercube sampling and Nataf transformation. In view of the nonlinear characteristics of power networks and gas networks, Chen *et al.* [16] applied multiple linearization methods to PEF calculation. Hu *et al.* [17] modeled the uncertainty of pipeline parameters as interval variables, modeled the uncertainty of electric/gas load and renewable power generation as probability variables, and proposed the probabilistic-interval energy flow analysis based on the polynomial chaos expansion method. In [18], wind speed and light intensity were defined as interval variables, load power of any node was defined as the random variable, and an uncertain power flow model of hybrid stochastic and interval variables was established and then solved by the double-layer Monte Carlo method. However, none of these studies considered the uncertainty of the distribution parameters of node power random variables in the PPF/PEF calculation, and it needs to be considered to reflect the uncertain fluctuations of node power more accurately.

In addition, there have been several studies in recent years on the analysis of power systems and integrated energy systems considering the higher-order uncertainty of node power. Lubin *et al.* [19], Zhou *et al.* [20] considered the uncertainty of the mean and variance of wind power in robust optimization models of power systems and combined heat and power systems, respectively. In [21], considering the uncertainty of the probability distribution type of wind power, a distributed robust coordinated scheduling model was proposed. Taking into account the uncertain characteristics of randomness and fuzziness, Wu *et al.* [22] proposed a random fuzzy power flow calculation method for distribution networks. It can be seen from the above studies that the existing research mainly focuses on the analysis of power systems considering higher-order uncertainty, whereas research on the analysis of integrated energy systems considering higher-order uncertainty is lacking. Moreover, there is still no literature on the PEF calculation of a CCHP-CMG considering higher-order uncertainty. Therefore, this paper focuses on the interval uncertainties of the distribution parameters of node power random variables in the CCHP-CMG and proposes an IPEF calculation method for CCHP-CMG.

This paper makes three contributions: 1) To reflect the uncertain fluctuations of node power including renewable energy station output and load power more accurate, intervals are used to describe the uncertainties of distribution parameters of node power random variables, and an IPEF calculation model of a CCHP-CMG is established considering the interval uncertainties of distribution parameters. An IA-based IPEF algorithm is proposed to solve this IPEF calculation model, and an interval Gram-Charlier expansion method is proposed to obtain the analytical expressions of PDF or CDF intervals of the state variables. 2) An AA&IA-based IPEF algorithm is proposed to address the interval extension problem and obtain more accurate IPEF calculation results. 3) By constructing correlation conversion matrixes to consider the correlation of load power and renewable energy station output, an AA&IA-based IPEF algorithm considering the correlation among different node power is proposed.

The rest of this paper is organized as follows. Section II introduces the IPEF calculation model of a CCHP-CMG considering the interval uncertainties of distribution parameters of node power random variables. Section III proposes an IA-based IPEF algorithm based on IA and cumulant method. Section IV proposes an AA&IA-based IPEF algorithm based on AA. Section V introduces an AA&IA-based IPEF algorithm considering the correlation among different node power. Section VI presents the case study and analysis of the results. Section VII offers the conclusions.

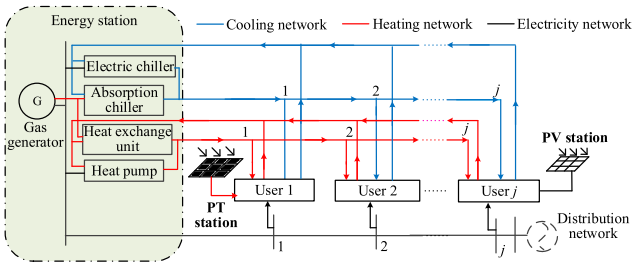

FIGURE 1. The structure and energy supply of a CCHP-CMG.

II. IPEF CALCULATION MODEL OF CCHP-CMG CONSIDERING THE INTERVAL UNCERTAINTIES OF DISTRIBUTION PARAMETERS

A. THE STRUCTURE OF A CCHP-CMG

The general structure and energy supply of a CCHP-CMG are shown in Fig. 1.

The CCHP-CMG contains gas generators, various cooling/heating equipment, distributed PV/PT stations, and electricity/heating/cooling networks. The gas is only the input energy of the gas generators, which is an external variable of the CCHP-CMG. In the proposed energy flow calculation, the CCHP unit is always set as the swing bus, and the input gas power can be calculated after obtaining the energy flow calculation result. Thus, the gas network is not considered in the energy flow calculation of this paper. In the energy station, there are CCHP units (gas generators, heat exchange units, and absorption chillers), heat pumps, and electric chillers. The energy station supplies power to users through gas generators and provides cooling and heating energy to users through cooling equipment (such as absorption chillers) and heating equipment (such as heat exchange units). Insufficient cooling/heating energy is supplemented by electric chillers or heat pumps. PV and PT stations can convert solar energy into electrical energy and heating energy, respectively, to supply power and heating users.

B. ENERGY FLOW CALCULATION MODEL OF CCHPCMG

1) HEATING/COOLING NETWORK

In the energy flow calculation, the state variables of the heating/cooling network include the flow rates of pipelines as well as the supply and return temperatures of the nodes, which satisfy the following equations [23]:

$$\begin{cases} \boldsymbol{\Phi}_{\mathrm{h/c}} = c_{\mathrm{w}} \boldsymbol{m}_{\mathrm{q.h/c}} s (T_{\mathrm{s.h/c}} - T_{\mathrm{r.h/c}}) \\ \boldsymbol{B}_{\mathrm{h/c}} \boldsymbol{D} \boldsymbol{m}_{\mathrm{h/c}} \left| \boldsymbol{m}_{\mathrm{h/c}} \right| = 0 \\ \boldsymbol{A}_{\mathrm{s.h/c}} \boldsymbol{T}_{\mathrm{s.h/c}} - \boldsymbol{b}_{\mathrm{s.h/c}} = 0 \\ \boldsymbol{A}_{\mathrm{r.h/c}} \boldsymbol{T}_{\mathrm{r.h/c}} - \boldsymbol{b}_{\mathrm{r.h/c}} = 0, \end{cases} \tag{1}$$

where the first formula is the expression of the node power of the heating/cooling network. For the pure heating/cooling load nodes, $\boldsymbol{\Phi}_{\mathrm{h/c}} = \boldsymbol{\Phi}_{\mathrm{L.h/c}}$, and for the heating load nodes connected to the PT station, $\boldsymbol{\Phi}_{\mathrm{h}} = \boldsymbol{\Phi}_{\mathrm{L.h}} - \boldsymbol{\Phi}_{\mathrm{PT}}$. The second formula is the pressure balance equation of pipelines. The third and fourth formulas are the balance equations for the supply and return temperatures of nodes, respectively.

2) ELECTRICITY NETWORK

The state variables of the electricity network are the voltage amplitude and phase angle of each bus, which satisfy the following equations:

$$\begin{cases} P_i = U_i \sum_{j=1}^{n} U_j (G_{ij} \cos \delta_{ij} + B_{ij} \sin \delta_{ij}) \\ Q_i = U_i \sum_{j=1}^{n} U_j (G_{ij} \sin \delta_{ij} - B_{ij} \cos \delta_{ij}), \end{cases} \tag{2}$$

where for the pure load bus, $P_i = -P_{\mathrm{L}i}$ and $Q_i = -Q_{\mathrm{L}i}$; for the load bus connected to the PV station, $P_i = P_{\mathrm{PV}i} - P_{\mathrm{L}i}$ and $Q_i = Q_{\mathrm{PV}i} - Q_{\mathrm{L}i}$.

3) COUPLING ELEMENTS

CCHP units can be divided into two types: back pressure units and extraction condensing units. The relationships between power output and wasted heat are respectively expressed as (3) and (4) [23]:

$$C_m = \Phi_{\mathrm{CCHP}} / P_{\mathrm{CCHP}}, \tag{3}$$

$$Z = \Phi_{\mathrm{CCHP}} \big/ (P_{\mathrm{CON}} - P_{\mathrm{CCHP}}). \tag{4}$$

The wasted heat can be converted into cooling/heating energy by the absorption chillers/heat exchangers, and the insufficient cooling/heat energy can be supplemented by the electric chillers/heat pumps. The above energy conversion elements all use the efficiency coefficient to perform energy conversion, as follows:

$$\Phi_{\mathrm{out}} = \eta_{\mathrm{E}} \Phi_{\mathrm{in}}. \tag{5}$$

According to (1)–(2), the energy flow equations can be abbreviated as follows:

$$\boldsymbol{F} = [\boldsymbol{W}; \boldsymbol{0}] = \boldsymbol{f}(\boldsymbol{X}) \tag{6}$$

For $\boldsymbol{W}$, the electrical/heating/cooling power at nodes of the energy station can be calculated by (3)–(5).

Given the network structure parameters and node power $\boldsymbol{W}$, equation (6) can be solved using the Newton-Raphson method to obtain the state variable $\boldsymbol{X}$ of the CCHP-CMG, which is the energy flow calculation of the CCHP-CMG.

C. REPRESENTATION OF HIGHER-ORDER UNCERTAINTY OF NODE POWER

In the traditional PEF algorithm, the distribution parameters in the PDF of the node power random variable are obtained from historical data, and these parameters are deterministic values. However, in practice, due to uncertain factors such as data absence and measurement errors, there are also uncertainties in the process of solving the distribution parameters of random variables. To express these uncertainties accurately, intervals are used to describe the uncertainties of the distribution parameters of node power random variables. Based on this concept, the IA-based IPEF algorithm of the CCHP-CMG is proposed.

Assuming that the electrical/heating/cooling load power W_{L} follows a normal distribution, its PDF is expressed as (7). Considering the uncertainties of μ_{L} and σ_{L}^2, they can be expressed by intervals as shown by (8).

$$f(W_{\mathrm{L}}) = \frac{1}{\sqrt{2\pi}\sigma_{\mathrm{L}}} \exp(-(W_{\mathrm{L}} - \mu_{\mathrm{L}})^2 \Big/ 2\sigma_{\mathrm{L}}^2). \tag{7}$$

$$\begin{cases} [\mu_{\mathrm{L}}] = [\underline{\mu}_{\mathrm{L}}, \bar{\mu}_{\mathrm{L}}] \\ [\sigma_{\mathrm{L}}^2] = [\underline{\sigma}_{\mathrm{L}}^2, \bar{\sigma}_{\mathrm{L}}^2]. \end{cases} \tag{8}$$

According to [12], [24], in calculating the power output of PV/PT stations, solar irradiance r is assumed to follow a β-distribution and its PDF is as follows:

$$f(r) = \frac{\Gamma(\alpha + \beta)}{\Gamma(\alpha)\Gamma(\beta)} (r/r_{\max})^{\alpha - 1} (1 - r/r_{\max})^{\beta - 1}, \tag{9}$$

where $\Gamma(\cdot)$ is the Gamma function.

Considering the uncertainties of the shape parameters α and β, they can be expressed by intervals as follows:

$$\begin{cases}[\alpha]=[\underline{\alpha},\bar{\alpha}]\\ [\beta]=[\underline{\beta},\bar{\beta}].\end{cases} \tag{10}$$

The relationship between the power output of a PV/PT station and the solar irradiance r is as follows:

$$\begin{cases}P_{\mathrm{PV}}=rA_{\mathrm{PV}}\eta_{\mathrm{PV}}\\ Q_{\mathrm{PV}}=rA_{\mathrm{PV}}\eta_{\mathrm{PV}}\tan\theta_{\mathrm{PV}}\\ \Phi_{\mathrm{PT}}=rA_{\mathrm{PT}}\eta_{\mathrm{PT}}.\end{cases} \tag{11}$$

The above (1)–(5) and (7)–(11) constitute the IPEF calculation model of the CCHP-CMG considering the interval uncertainties of distribution parameters.

III. IPEF ALGORITHM BASED ON INTERVAL ARITHMETIC

A. PEF ALGORITHM BASED ON CUMULANT METHOD

In the PEF calculation considering the randomness of node power, the given node power and unknown state variables are represented by random variables. Equation (6) is expanded by the Taylor series, and only the constant term and the first-order term are retained to obtain the linearized energy flow equations as follows:

$$\begin{aligned}\boldsymbol{F}_0+\Delta\boldsymbol{F}&=[\boldsymbol{W}_0;\boldsymbol{0}]+[\Delta\boldsymbol{W};\boldsymbol{0}]\\ &=\boldsymbol{f}(\boldsymbol{X}_0+\Delta\boldsymbol{X})=\boldsymbol{f}(\boldsymbol{X}_0)+\boldsymbol{J}\Delta\boldsymbol{X}.\end{aligned} \tag{12}$$

Each element of the Jacobian matrix $\boldsymbol{J}$ is the partial derivative of the energy flow equations with respect to the state variables (i.e., $\boldsymbol{J}=\partial\boldsymbol{f}(\boldsymbol{X})/\partial\boldsymbol{X}$).

After the steady-state reference value of energy flow $\boldsymbol{F}_0=\boldsymbol{f}(\boldsymbol{X}_0)$ is substituted into (12), equation (13) can be obtained.

$$\Delta\boldsymbol{X}=\boldsymbol{J}^{-1}[\Delta\boldsymbol{W};\boldsymbol{0}]=\boldsymbol{S}_0[\Delta\boldsymbol{W};\boldsymbol{0}]=\boldsymbol{S}_0\Delta\boldsymbol{F}, \tag{13}$$

where the sensitivity matrix $\boldsymbol{S}_0=\boldsymbol{J}^{-1}$.

Applying the cumulant method to the PEF calculation of the CCHP-CMG, the steps are as follows. According to the PDFs and the distribution parameters of $\Delta\boldsymbol{W}$, the cumulants of $\Delta\boldsymbol{W}$ are obtained. These cumulants are combined with the calculated $\boldsymbol{S}_0^{<k>}$ and then substituted into (14) to obtain the cumulants of $\Delta\boldsymbol{X}$. Finally, the PDFs or CDFs of $\boldsymbol{X}$ are obtained by the Gram-Charlier expansion [11].

$$\boldsymbol{\gamma}_{\Delta\mathrm{X}}^{(k)}=\boldsymbol{S}_0^{<k>}[\boldsymbol{\gamma}_{\Delta\mathrm{W}}^{(k)};\boldsymbol{0}]. \tag{14}$$

B. IPEF ALGORITHM BASED ON INTERVAL ARITHMETIC AND CUMULANT METHOD

In the PEF calculation, considering the distribution parameter uncertainties, the distribution parameters of random variables of node power are expressed as intervals. Then, the cumulants of node power calculated according to the distribution parameter intervals are also the intervals, called the cumulant intervals (CIs). The CIs of $\Delta\boldsymbol{X}$ can be obtained from (14). Finally, the analytical expressions of the PDF and CDF intervals of state variables $\boldsymbol{X}$ are obtained by the proposed interval Gram-Charlier expansion method.

1) CALCULATION OF THE CUMULANT INTERVALS OF NODE POWER AND STATE VARIABLES

According to IA [25], given the intervals $[x]=[\underline{x},\bar{x}]$ and $[y]=[\underline{y},\bar{y}]$, we have:

$$\text{addition:}[x]+[y]=[\underline{x}+\underline{y},\bar{x}+\bar{y}], \tag{15}$$

$$\text{subtraction:}[x]-[y]=[\underline{x}-\bar{y},\bar{x}-\underline{y}], \tag{16}$$

$$\text{multiplication:}\begin{cases}[x]\cdot[y]=[\min S,\max S]\\ S=\{\underline{x}\underline{y},\underline{x}\bar{y},\bar{x}\underline{y},\bar{x}\bar{y}\},\end{cases} \tag{17}$$

$$\text{division:}\begin{cases}[x]\big/[y]=[\min R,\max R]\\ R=\{\underline{x}/\underline{y},\underline{x}/\bar{y},\bar{x}\big/\underline{y},\bar{x}/\bar{y}\}.\end{cases} \tag{18}$$

For the electric/heating/cooling load power that follows the normal distribution, the first-order and second-order CIs are their mean and variance values, respectively. Any CIs above the second order are equal to zero, as shown in (19).

$$\begin{cases}[\gamma_{\mathrm{L.e/h/c}}^{(1)}]=[\boldsymbol{\mu}_{\mathrm{L}}]\\ [\gamma_{\mathrm{L.e/h/c}}^{(2)}]=[\boldsymbol{\sigma}_{\mathrm{L}}^2]\\ [\gamma_{\mathrm{L.e/h/c}}^{(k)}]=\boldsymbol{0}\qquad k\geq 3\end{cases} \tag{19}$$

The CIs of the power output of PV/PT stations can be obtained from the CIs of the solar irradiance r. According to the standard β-distribution, the recursive formula of the origin moment intervals of r is as follows

$$\begin{cases}[M_{\mathrm{r}}^{(1)}]=\dfrac{[\alpha]}{[\alpha]+[\beta]}\\ [M_{\mathrm{r}}^{(k)}]=\dfrac{[\alpha]+(k-1)}{[\alpha]+[\beta]+(k-1)}[M_{\mathrm{r}}^{(k-1)}]\quad k\geq 2\end{cases} \tag{20}$$

Each order CI of r is obtained from the origin moment interval, as in (21).

$$\begin{cases}[\gamma_{\mathrm{r}}^{(1)}]=[M_{\mathrm{r}}^{(1)}]\\ [\gamma_{\mathrm{r}}^{(k)}]=[M_{\mathrm{r}}^{(k)}]+\sum_{i=1}^{k-1}C_{k-1}^{i}[M_{\mathrm{r}}^{(i)}][\gamma_{\mathrm{r}}^{(k-i)}]\quad k\geq 2\end{cases} \tag{21}$$

According to the relationship between the power output of a PV/PT station and the solar irradiance r (i.e., (11)), from the k-order CI of r (i.e., $[\gamma_r^{(\mathrm{k})}]$), the k-order CI of the power output of PV/PT stations can be calculated as (22).

$$\begin{cases}[\boldsymbol{\gamma}_{\mathrm{PPV}}^{(k)}]=(\boldsymbol{A}_{\mathrm{PV}}\boldsymbol{\eta}_{\mathrm{PV}})^{<k>}[\gamma_{\mathrm{r}}^{(k)}]\\ [\boldsymbol{\gamma}_{\mathrm{QPV}}^{(k)}]=(\boldsymbol{A}_{\mathrm{PV}}\boldsymbol{\eta}_{\mathrm{PV}}\tan\theta_{\mathrm{PV}})^{<k>}[\gamma_{\mathrm{r}}^{(k)}]\\ [\boldsymbol{\gamma}_{\mathrm{PT}}^{(k)}]=(\boldsymbol{A}_{\mathrm{PT}}\boldsymbol{\eta}_{\mathrm{PT}})^{<k>}[\gamma_{\mathrm{r}}^{(k)}]\end{cases} \tag{22}$$

Based on the mean value, the CIs of the random fluctuation of electric/heating/cooling load power and PV/PT station power output can be calculated as follows:

$$\begin{cases}[\boldsymbol{\gamma}_{\Delta\mathrm{L.e/h/c}}^{(1)}]=[\boldsymbol{\gamma}_{\mathrm{L.e/h/c}}^{(1)}]-\boldsymbol{\mu}_{\mathrm{L}}\\ [\boldsymbol{\gamma}_{\Delta\mathrm{L.e/h/c}}^{(k)}]=[\boldsymbol{\gamma}_{\mathrm{L.e/h/c}}^{(k)}],\quad(k\geq 2)\\ [\boldsymbol{\gamma}_{\Delta\mathrm{PV}}^{(1)}]=[\boldsymbol{\gamma}_{\mathrm{PV}}^{(1)}]-\boldsymbol{\mu}_{\mathrm{PV}}\\ [\boldsymbol{\gamma}_{\Delta\mathrm{PV}}^{(k)}]=[\boldsymbol{\gamma}_{\mathrm{PV}}^{(k)}],\qquad(k\geq 2)\\ [\boldsymbol{\gamma}_{\Delta\mathrm{PT}}^{(1)}]=[\boldsymbol{\gamma}_{\mathrm{PT}}^{(1)}]-\boldsymbol{\mu}_{\mathrm{PT}}\\ [\boldsymbol{\gamma}_{\Delta\mathrm{PT}}^{(k)}]=[\boldsymbol{\gamma}_{\mathrm{PT}}^{(k)}],\qquad(k\geq 2),\end{cases} \tag{23}$$

where $[\boldsymbol{\gamma}_{\mathrm{PV}}^{(k)}]=\left[[\boldsymbol{\gamma}_{\mathrm{PPV}}^{(k)}];[\boldsymbol{\gamma}_{\mathrm{QPV}}^{(k)}]\right]$.

If the PV/PT stations are connected to the load buses/nodes of the electricity/heating network, the CIs of the injected power of these buses/nodes in the CCHP-CMG can be obtained as follows:

$$\begin{cases} [\boldsymbol{\gamma}^{(k)}_{\Delta \mathrm{W.e}}] = [\boldsymbol{\gamma}^{(k)}_{\Delta \mathrm{PV}}] - [\boldsymbol{\gamma}^{(k)}_{\Delta \mathrm{L.e}}] \\ [\boldsymbol{\gamma}^{(k)}_{\Delta \mathrm{W.h}}] = [\boldsymbol{\gamma}^{(k)}_{\Delta \mathrm{PT}}] - [\boldsymbol{\gamma}^{(k)}_{\Delta \mathrm{L.h}}] \\ [\boldsymbol{\gamma}^{(k)}_{\Delta \mathrm{W.c}}] = -[\boldsymbol{\gamma}^{(k)}_{\Delta \mathrm{L.c}}]. \end{cases} \tag{24}$$

Thus, the CIs of $\Delta \boldsymbol{X}$ can be obtained as follows:

$$[\boldsymbol{\gamma}^{(k)}_{\Delta \mathrm{X}}] = \boldsymbol{S}_0^{<k>} \begin{bmatrix} [\boldsymbol{\gamma}^{(k)}_{\Delta \mathrm{W}}] \\ \mathbf{0} \end{bmatrix}, \tag{25}$$

where $[\boldsymbol{\gamma}^{(k)}_{\Delta \mathrm{W}}] = \left[[\boldsymbol{\gamma}^{(k)}_{\Delta \mathrm{W.e}}]; [\boldsymbol{\gamma}^{(k)}_{\Delta \mathrm{W.h}}]; [\boldsymbol{\gamma}^{(k)}_{\Delta \mathrm{W.c}}] \right]$.

The reference values $\boldsymbol{X}_0$ calculated from the steady-state energy flow calculation can be used to obtain the k-order CI vector $[\boldsymbol{\gamma}^{(k)}_{\mathrm{X}}]$ of state variables $\boldsymbol{X}$, as follows:

$$\begin{cases} [\boldsymbol{\gamma}^{(1)}_{\mathrm{X}}] = [\boldsymbol{\gamma}^{(1)}_{\Delta \mathrm{X}}] + \boldsymbol{X}_0 \\ [\boldsymbol{\gamma}^{(k)}_{\mathrm{X}}] = [\boldsymbol{\gamma}^{(k)}_{\Delta \mathrm{X}}] \qquad (k \geq 2) \end{cases} \tag{26}$$

2) INTERVAL GRAM-CHARLIER EXPANSION

After obtaining the CIs of $\boldsymbol{X}$, this paper proposes an interval Gram-Charlier expansion method based on the traditional Gram-Charlier expansion method, which can expand the CIs of $\boldsymbol{X}$ to obtain the analytical expressions of the PDF and CDF intervals of $\boldsymbol{X}$.

After the calculation of the CIs of state variables $\boldsymbol{X}$, the mean interval $[\mu]$ and standard deviation interval $[\sigma]$ of $\boldsymbol{X}$ are known, and the random variable must first be standardized:

$$[\tilde{x}] = (x - [\mu]) \big/ [\sigma], \tag{27}$$

where x is the value of the random variable X, and $[\tilde{x}]$ is the interval value of the standardized random variable $\tilde{X}$.

Assuming that $[y_{\tilde{X}}]$ and $[Y_{\tilde{X}}]$ are the PDF and CDF intervals of $\tilde{X}$, according to the Gram-Charlier expansion, the PDF interval and CDF interval can be expanded into the series as follows:

$$[y_{\tilde{X}}] = [\varphi([\tilde{x}])] + \frac{[g_1]}{1!}[\varphi^{(1)}([\tilde{x}])] + \frac{[g_2]}{2!}[\varphi^{(2)}([\tilde{x}])] + \cdots + \frac{[g_k]}{k!}[\varphi^{(k)}([\tilde{x}])], \tag{28}$$

$$[Y_{\tilde{X}}] = [\Phi([\tilde{x}])] + \frac{[g_1]}{1!}[\Phi^{(1)}([\tilde{x}])] + \frac{[g_2]}{2!}[\Phi^{(2)}([\tilde{x}])] + \cdots + \frac{[g_k]}{k!}[\Phi^{(k)}([\tilde{x}])]. \tag{29}$$

Since $[\tilde{x}]$ is an interval, the PDF and CDF calculated from (28)–(29) are also intervals.

In (28)–(29), $[\varphi([\tilde{x}])]$ and $[\Phi([\tilde{x}])]$ are the intervals obtained from the PDF and CDF formulas of the standard normal distribution; $[\varphi^{(k)}([\tilde{x}])]$ and $[\Phi^{(k)}([\tilde{x}])]$ are the k-th derivatives of $[\varphi([\tilde{x}])]$ and $[\Phi([\tilde{x}])]$, respectively. These variables can be obtained by (30)–(31):

$$\begin{cases} [\varphi([\tilde{x}])] = 1 \Big/ \sqrt{2\pi} \exp(-[\tilde{x}]^2/2) & k = 1 \\ [\varphi^{(k)}([\tilde{x}])] = (-1)^{(k)} [H_k([\tilde{x}])][\varphi([\tilde{x}])] & k \geq 2, \end{cases} \tag{30}$$

$$\begin{cases} [\Phi([\tilde{x}])] = 1 \Big/ \sqrt{2\pi} \int_{-\infty}^{[\tilde{x}]} \exp(-t^2/2) dt & k = 1 \\ [\Phi^{(k)}([\tilde{x}])] = [\varphi^{(k-1)}([\tilde{x}])] & k \geq 2 . \end{cases} \tag{31}$$

In (30), $[H_k([\tilde{x}])]$ is the k-order Hermite polynomial interval, as follows:

$$\begin{cases} [H_0([\tilde{x}])] = 1 \\ [H_1([\tilde{x}])] = [\tilde{x}] \\ [H_2([\tilde{x}])] = [\tilde{x}]^2 - 1 \\ [H_3([\tilde{x}])] = [\tilde{x}]^3 - 3[\tilde{x}] \\ [H_4([\tilde{x}])] = [\tilde{x}]^4 - 6[\tilde{x}]^2 + 3 \\ [H_5([\tilde{x}])] = [\tilde{x}]^5 - 10[\tilde{x}]^3 + 15[\tilde{x}] \\ [H_6([\tilde{x}])] = [\tilde{x}]^6 - 15[\tilde{x}]^4 + 45[\tilde{x}]^2 - 15 \\ [H_7([\tilde{x}])] = [\tilde{x}]^7 - 21[\tilde{x}]^5 + 105[\tilde{x}]^3 - 105[\tilde{x}] \\ \vdots \end{cases} \tag{32}$$

According to equations (19)–(26), the k-th order CI $[\gamma^{(k)}_X]$ of X is obtained, and then each coefficient in (28)–(29) can be obtained as follows:

$$[g_k] = [\gamma^{(k)}_X] \big/ [\sigma]^k, \tag{33}$$

where $[\sigma]^k$ is the k-th power of $[\sigma]$.

Finally, the PDF and CDF intervals of $\boldsymbol{X}$ can be obtained as follows:

$$[y_X] = [y_{\tilde{X}}] \big/ [\sigma], \tag{34}$$

$$[Y_X] = [Y_{\tilde{X}}], \tag{35}$$

where $[y_X]$ and $[Y_X]$ are the PDF and CDF intervals of X.

It can be seen that equations (28), (30), (32), (33), and (34) constitute the analytical expressions of the PDF interval of $\boldsymbol{X}$; equations (29), (31), (32), (33), and (35) constitute the analytical expressions of the CDF interval of $\boldsymbol{X}$. The above (27)–(35) constitute the proposed interval Gram-Charlier expansion method.

IV. AA&IA-BASED IPEF ALGORITHM FOR ADDRESSING THE INTERVAL EXTENSION PROBLEM

Due to interval dependency, the interval extension problem inevitably exists in the process of interval arithmetic [25], which leads to an excessive fluctuation interval of the calculation result. To solve this problem, affine arithmetic (AA) is introduced to the IA-based IPEF algorithm. According to AA, the value of an uncertain variable $x \in [\underline{x}, \bar{x}]$ is affected by itself and the independent noises of the environment, which is expressed as an affine form [26]:

$$\hat{x} = x_0 + x_1\varepsilon_1 + \cdots x_k\varepsilon_k, \tag{36}$$

where x_0 is the central value (i.e., $x_0 = (\underline{x} + \bar{x})/2$), $\varepsilon_i \in [-1, 1]$ is the i-th independent noise element, and the coefficient $x_i \in R$ is the i-th partial increment.

According to AA theory, the interval form and affine form of an uncertain variable can be transformed to each other.

Given an affine form as in (36), the corresponding interval form is:

$$[\underline{x}, \bar{x}] = [x_0 - \xi, x_0 + \xi], \quad \xi = \sum_{i=1}^{k} |x_i|. \tag{37}$$

Given an interval form $[x] = [\underline{x}, \bar{x}]$, let $a = (\underline{x} + \bar{x})/2$ and $b = (\bar{x} - \underline{x})/2$; then the corresponding affine form is:

$$\hat{x} = a + b\varepsilon_1. \tag{38}$$

Given two affine forms $\hat{x} = x_0 + x_1\varepsilon_1 + \cdots + x_k\varepsilon_k$ and $\hat{y} = y_0 + y_1\varepsilon_1 + \cdots + y_k\varepsilon_k$, the AA rules are as follows:

$$\begin{aligned}
&① \ \hat{x} \pm \hat{y} = (x_0 \pm y_0) + (x_1 \pm y_1)\varepsilon_1 + \cdots + (x_k \pm y_k)\varepsilon_k \\
&② \ \hat{x} \cdot \hat{y} = x_0 y_0 + \sum_{i=1}^{k} (x_0 y_i + y_0 x_i)\varepsilon_i \\
&\qquad + (\sum_{i=1}^{k} x_i\varepsilon_i) \cdot (\sum_{i=1}^{k} y_i\varepsilon_i) \\
&③ \ \hat{x}/\hat{y} = \hat{x} \cdot (1/\hat{y}).
\end{aligned} \tag{39}$$

Compared with IA, the AA can consider the interval dependency and identify itself in the computation, which can effectively avoid the interval extension problem. However, the calculation of AA is more complicated than that of IA, hence its calculation speed is slower, which has an adverse effect on the solution of the IPEF. In addition, in the IA-based IPEF algorithm, only part of the calculation process will result in a large interval extension problem due to IA. They are mainly in the following two calculation processes: First, in the calculation of the CIs of solar irradiance, the numerator and denominator of (20) contain the same interval $[\alpha]$. Since IA cannot identify itself, interval extension will inevitably occur. Moreover, in (20), there is a recursive process of intervals when calculating the k-th order origin moment interval from the $(k-1)$-th order origin moment interval, so the interval extension will accumulate in the layer-by-layer recursive process. Second, in the interval Gram-Charlier expansion method, there is also the calculation of the interval and itself in (32), which will also lead to interval extension. Therefore, to further improve the IA-based IPEF algorithm, an AA&IA-based IPEF algorithm is proposed. In this algorithm, the AA is introduced to calculate the CIs of solar irradiance and is applied in the interval Gram-Charlier expansion, whereas the other calculation steps are still solved with IA. This algorithm can address the interval extension problem caused by IA and obtain more accurate analytical expressions of the PDF and CDF intervals of $\boldsymbol{X}$.

V. IPEF CALCULATION OF CCHP-CMG CONSIDERING THE CORRELATION AMONG NODE POWER

In actual CCHP-CMGs, there is obvious correlation among the power output of distributed renewable energy stations. For example, the power output of different PV stations and PT stations is affected by solar irradiance and has correlation. Besides, the electrical/heating/cooling load power of different buses/nodes may also be relevant. Therefore, in the IPEF calculation of a CCHP-CMG, the correlation among the load power of different buses/nodes and the power output of different renewable energy stations need to be considered.

A. CORRELATION CONVERSION MATRIX K

If there are n elements in the vector $\boldsymbol{F}$, it can be assumed that m elements of $\boldsymbol{F}$ are relevant and form a vector $\boldsymbol{V}$, and the other elements are not relevant. The calculation steps of the correlation conversion matrix $\boldsymbol{K}$ are as follows:

1) If the correlation coefficient matrix of each element in $\boldsymbol{V}$ is known as $\boldsymbol{C}_\mathrm{r}$, and the standard deviation vector of each element in $\boldsymbol{V}$ is known as σ_V, the covariance matrix $\boldsymbol{C}_\mathbf{v}$ can be obtained by the following:

$$C_\mathrm{v}(i,j) = C_\mathrm{r}(i,j) \cdot \sigma_{\mathrm{V}i} \cdot \sigma_{\mathrm{V}j}, \tag{40}$$

where $C_\mathrm{v}(i,j)$ and $C_\mathrm{r}(i,j)$ are respectively the i-th row and j-th column elements of matrixes $\boldsymbol{C}_\mathrm{v}$ and $\boldsymbol{C}_\mathrm{r}$; $\sigma_{\mathrm{V}i}$ and $\sigma_{\mathrm{V}j}$ are respectively the standard deviations of the i-th and j-th variables in the vector $\boldsymbol{V}$.

2) Apply the Cholesky decomposition to the covariance matrix $\boldsymbol{C}_\mathrm{v}$ to obtain the lower triangular matrix $\boldsymbol{G}$ [13].

3) The correlation conversion matrix $\boldsymbol{K}$ can be obtained from (41):

$$\begin{aligned}
&① \ if \ (F_i \to V_k) \wedge (F_j \to V_l) \ \Rightarrow \begin{cases} K_{ii} = G_{kk}, K_{jj} = G_{ll} \\ K_{ij} = G_{kl}, K_{ji} = G_{lk} \end{cases} \\
&② \ else \begin{cases} K_{ii} = 1, \\ K_{ij} = K_{ji} = 0 \end{cases} \\
&\qquad \text{(other elements in } \boldsymbol{K} \text{ except those in①)}
\end{aligned} \tag{41}$$

where $F_i \to V_k$ and $F_j \to V_l$ mean that the i-th and j-th elements in $\boldsymbol{F}$ are correlation variables and correspond to the k-th and l-th elements in $\boldsymbol{V}$, respectively. Additionally, $k, \ l \in [1, 2, \ldots, m]$, $i, j \in [1, 2, \ldots, n]$.

Since the standard deviations of node power of different buses/nodes are intervals, the covariance matrix is an interval matrix $[\boldsymbol{C}_\mathbf{v}]$. However, the Cholesky decomposition of the interval matrix can only find the interval matrix $[\boldsymbol{G}]$ to satisfy (42) [27]. It can be seen that (42) is an inclusion relation rather than a strict equality relation, so the interval matrix $[\boldsymbol{G}]$ will cause the interval extension problem for subsequent calculations. The existing improved methods are very complicated, have longer calculation time, or do not meet the requirements of the solution in this paper [28], [29]. Therefore, this paper considers using the central values of the standard deviation intervals to constitute the ordinary covariance matrix $\boldsymbol{C}_\mathbf{v}$ and calculate the matrix $\boldsymbol{K}$ to consider the correlation problem. The results of the subsequent case study show that this simplified step does not cause obvious calculation errors.

$$[\boldsymbol{C}_v] \subseteq [\boldsymbol{G}][\boldsymbol{G}]^T. \tag{42}$$

B. IPEF CALCULATION METHOD OF CCHP-CMG CONSIDERING NODE POWER CORRELATION

In the IPEF calculation of a CCHP-CMG considering the node power correlation, the random fluctuation of the node power augmented vector $\Delta\boldsymbol{F}$ in (13) can be divided into the following two parts:

$$\Delta\boldsymbol{F} = \Delta\boldsymbol{F}_\mathrm{S} - \Delta\boldsymbol{F}_\mathrm{L}, \tag{43}$$

where $\Delta \boldsymbol{F}_{\mathrm{L}}$ and $\Delta \boldsymbol{F}_{\mathrm{S}}$ have the following relationship:

$$\begin{cases} \Delta \boldsymbol{F}_{\mathrm{L}} = \boldsymbol{K}_{\mathrm{L}} \Delta \boldsymbol{F}'_{\mathrm{L}} \\ \Delta \boldsymbol{F}_{\mathrm{S}} = \boldsymbol{K}_{\mathrm{S}} \Delta \boldsymbol{F}'_{\mathrm{S}}. \end{cases} \tag{44}$$

If the CIs of $\Delta \boldsymbol{F}_{\mathrm{L}}$ and $\Delta \boldsymbol{F}_{\mathrm{S}}$ are $[\boldsymbol{\gamma}_{\Delta FL}^{(k)}]$ and $[\boldsymbol{\gamma}_{\Delta FS}^{(k)}]$, they can be de-correlated by the following formula:

$$\begin{cases} [\boldsymbol{\gamma}'_{\Delta \mathrm{FL}}{}^{(k)}] = (\boldsymbol{K}_{\mathrm{L}}^{<k>})^{-1} [\boldsymbol{\gamma}_{\Delta \mathrm{FL}}^{(k)}] \\ [\boldsymbol{\gamma}'_{\Delta \mathrm{FS}}{}^{(k)}] = (\boldsymbol{K}_{\mathrm{S}}^{<k>})^{-1} [\boldsymbol{\gamma}_{\Delta \mathrm{FS}}^{(k)}]. \end{cases} \tag{45}$$

Substituting (43)–(44) into (13):

$$\begin{aligned} \Delta \boldsymbol{X} &= \boldsymbol{S}_0 \Delta \boldsymbol{F} = \boldsymbol{S}_0 (\Delta \boldsymbol{F}_{\mathrm{S}} - \Delta \boldsymbol{F}_{\mathrm{L}}) \\ &= \boldsymbol{S}_0 \boldsymbol{K}_{\mathrm{S}} \Delta \boldsymbol{F}'_{\mathrm{S}} - \boldsymbol{S}_0 \boldsymbol{K}_{\mathrm{L}} \Delta \boldsymbol{F}'_{\mathrm{L}}. \end{aligned} \tag{46}$$

Then, the CIs of the fluctuation of state variables $\Delta \boldsymbol{X}$ can be obtained by the following equation:

$$[\boldsymbol{\gamma}_{\Delta \mathrm{X}}^{(k)}] = (\boldsymbol{S}_0 \boldsymbol{K}_{\mathrm{S}})^{<k>} [\boldsymbol{\gamma}'_{\Delta \mathrm{FS}}{}^{(k)}] - (\boldsymbol{S}_0 \boldsymbol{K}_{\mathrm{L}})^{<k>} [\boldsymbol{\gamma}'_{\Delta \mathrm{FL}}{}^{(k)}]. \tag{47}$$

Therefore, by replacing (25) in Section III with (45) and (47) in Section V, based on the original AA&IA-based IPEF algorithm, an AA&IA-based IPEF algorithm considering the node power correlation is proposed. The flowchart of the algorithm is shown in Fig. 2. The shaded rectangular boxes of solid and dotted lines are respectively calculated by IA and AA.

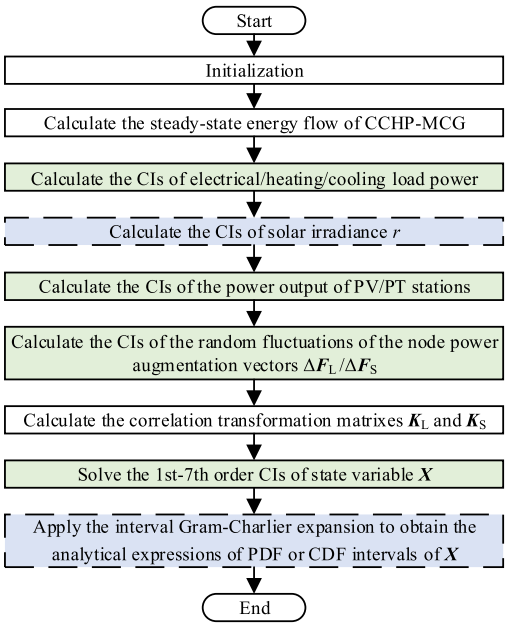

FIGURE 2. Flowchart of the AA&IA-based IPEF algorithm considering the node power correlation.

The calculation steps are as follows:

1) Initialization: Determine the probability distribution models of electrical/heating/cooling load power and solar irradiance, the intervals of the distribution parameters, and the correlation coefficient matrix $\boldsymbol{C}_{\mathrm{r}}$ of the relevant node power.
2) Calculate the steady-state energy flow of the CCHP-CMG. The result is used as a reference.
3) Apply IA to calculate the CIs of electrical/heating/cooling load power. Meanwhile, apply AA to calculate the CIs of the solar irradiance, and apply IA to calculate the CIs of the power output of PV/PT stations.
4) Calculate the CIs of the random fluctuations of the node power augmented vectors $\Delta \boldsymbol{F}_{\mathrm{L}}/\Delta \boldsymbol{F}_{\mathrm{S}}$.
5) Calculate the correlation conversion matrixes $\boldsymbol{K}_{\mathrm{L}}$ and $\boldsymbol{K}_{\mathrm{S}}$ of the node power of loads and renewable energy stations.
6) The CIs of the state variable $\boldsymbol{X}$ are solved according to (26), (45), and (47), and the analytical expressions of PDF or CDF intervals of $\boldsymbol{X}$ can be obtained by the interval Gram-Charlier expansion as (27)–(35).

VI. CASE STUDY

The structure of a CCHP-MCG is shown in Fig. 3, which is divided into two energy supply areas with three energy stations. In this CCHP-MCG, the electricity network is a distribution network of an actual industrial campus and the cooling and heating networks are improved based on the heating network in [23]. The energy coupling components in the energy stations include CCHP units (gas-fired power generators, heat exchange units, and absorption chillers), heat pumps, and electric chillers. The cooling and heating networks have the same structure, including 49 nodes and 49 pipelines. The energy stations I/II/III are respectively located at the 49$^{\mathrm{th}}$, 48$^{\mathrm{th}}$, and 47$^{\mathrm{th}}$ nodes of the cooling/heating network. Among them, energy stations I and II are respectively assumed to be the swing nodes of the heating network and cooling network. The electricity network contains 91 buses. Energy stations I/II/III are respectively located at the 90$^{\mathrm{th}}$, 89$^{\mathrm{th}}$, and 91$^{\mathrm{st}}$ buses of the electricity network. Generator buses in the energy stations I/II/III are assumed to be PV buses. The 88$^{\mathrm{th}}$ bus connected to the public distribution network is set to be the swing bus, and the remaining buses are all PQ buses. The generated electric power values of the CCHP units in energy stations I/II/III are determined by their wasted heating power. The CCHP units in energy stations I and III are the back pressure units, and the CCHP units in energy station II are the extraction condensing units.

The PV and PT stations are respectively connected to the load buses/nodes of the electricity and heating network. It is assumed that the solar irradiance follows the β-distribution. Using the historical data in Guangzhou City, Guangdong Province, China (23°6′ N, 113°2′ E), the shape parameters of the probability distribution of the solar irradiance are obtained by fitting, the central values of $[\alpha]$ and $[\beta]$ are taken as 0.6798 and 1.7788, respectively [30], and the interval radii are 0.1% of the central values. The total power output of PV stations accounts for 15% of the electrical load power, and the total power output of PT stations accounts for 5% of the heating load power. In addition, the electricity/heating/cooling load in the CCHP-CMG is assumed to follow a normal distribution. The central value of the mean interval $[\mu]$ takes the

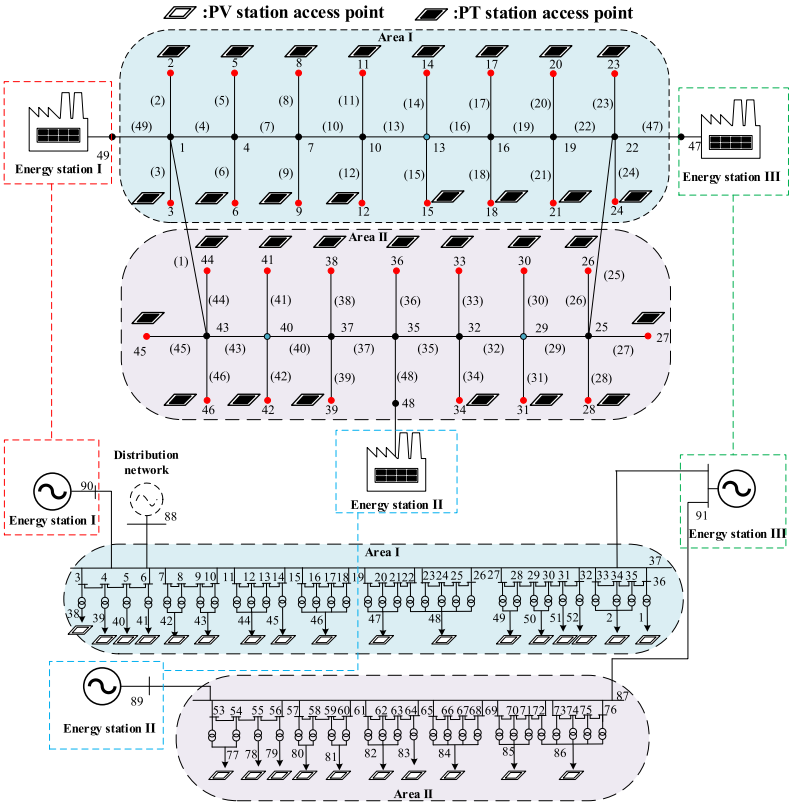

FIGURE 3. The structure of the case-study CCHP-CMG.

steady-state power flow state values, and the interval radius of $[\mu]$ is 0.2% of the center value. The standard deviation interval of electrical power is 10% $[\mu]$, and the standard deviation interval of heating/cooling power is 5% $[\mu]$.

All of the numerical calculation tests are performed on a PC with Intel(R) Core(TM) CPU i7-8700 3.20 GHz and 32 GB RAM. The proposed algorithms are coded in MATLAB programs, which use INTLAB toolbox for IA and AA [31].

A. ANALYSIS OF CALCULATION RESULT

In addition to the affine arithmetic, another common improved interval method to address the interval extension problem is the interval subdivision method [25]. The interval division method is applied to calculate the CIs of solar irradiance and the interval Gram-Charlier expansion, and the IPEF algorithm based on interval subdivision and interval arithmetic (IS&IA-based IPEF algorithm) is proposed as a comparison with the AA&IA-based IPEF algorithm. Then, the IA-based IPEF algorithm, AA&IA-based IPEF algorithm, IS& IA-based IPEF algorithm, and double-layer Monte Carlo (DMC) method are each used to solve the IPEF problem in the CCHP-CMG. In the DMC method, assuming the distribution parameters follow a uniform distribution in their uncertain fluctuation intervals, the distribution parameter values of node power random variables are obtained by outer-layer sampling, and the sampling number is 1,000. After determining the distribution parameter values to obtain the PDFs of node power, the node power values are obtained by inner-layer sampling, and the sampling number is 10,000. Each sample of node power values is substituted into the energy flow calculation to obtain the state variable values. In the AA&IA-based, IS&IA-based and IA-based IPEF algorithms, only the 1^{st}–7^{th} order CIs are calculated, and it can ensure the results with sufficient accuracy for these algorithms. In the IS&IA-based IPEF algorithm, the intervals are divided into 100 subintervals.

With the calculation results of the DMC method as a reference, the calculation accuracies of the proposed three algorithms are compared and verified. Taking the voltage phase angle and amplitude at bus-2 of the electricity network, the flow rate of pipe-2, and the supply temperature at node-2 of the heating network as examples, the CIs obtained by different algorithms are shown in Table 1. Method I, Method II and Method III refer to the AA&IA-based IPEF algorithm, the IS&IA-based IPEF algorithm and the IA-based IPEF algorithm. The above CIs are used to obtain the analytical expressions of PDF or CDF intervals of state variables by the interval Gram-Charlier expansion. Then, the upper and lower bounds of the PDF or CDF curves of state variables can also be obtained. For the above state variables, the upper and lower bounds of the CDF curves are compared with the

TABLE 1. Each order CI of several state variables.

Order		1	2	3	4	5	6	7
δ_2	I	[-0.024,-0.020]	[3.43,3.54]*10^{-5}	[5.50,5.51]*10^{-8}	[-6.09,-5.86]*10^{-11}	[-3.15,-3.13]*10^{-12}	[-2.06,-2.04]*10^{-14}	[2.72,2.77]*10^{-16}
	II	[-0.024,-0.020]	[3.43,3.55]*10^{-5}	[5.32,5.69]*10^{-8}	[-1.06,-0.14]*10^{-10}	[-4.61,-1.66]*10^{-12}	[-7.96,3.87]*10^{-14}	[-2.58,3.13]*10^{-15}
	III	[-0.024,-0.020]	[3.41,3.57]*10^{-5}	[5.04,5.97]*10^{-8}	[-1.73,0.53]*10^{-10}	[-6.77,0.50]*10^{-12}	[-1.66,1.26]*10^{-13}	[-6.76,7.32]*10^{-15}
U_2	I	[1.023,1.024]	[9.60,9.91]*10^{-6}	[1.14,1.15]*10^{-8}	[-8.15,-7.85]*10^{-12}	[-2.60,-2.58]*10^{-13}	[-1.04,-1.03]*10^{-15}	[8.34,8.52]*10^{-18}
	II	[1.023,1.024]	[9.58,9.93]*10^{-6}	[1.11,1.19]*10^{-8}	[-1.42,-0.18]*10^{-11}	[-3.81,-1.37]*10^{-13}	[-4.02,1.96]*10^{-15}	[-7.91,9.61]*10^{-17}
	III	[1.023,1.024]	[9.53,9.98]*10^{-6}	[1.05,1.25]*10^{-8}	[-2.32,0.71]*10^{-11}	[-5.60,0.42]*10^{-13}	[-8.39,6.34]*10^{-15}	[-2.08,2.25]*10^{-16}
m_{h2}	I	[0.951,0.992]	[4.38,4.59]*10^{-3}	[-7.08,-7.06]*10^{-5}	[-9.40,-9.05]*10^{-7}	[5.53,5.56]*10^{-7}	[-4.11,-4.07]*10^{-8}	[-6.21,-6.08]*10^{-9}
	II	[0.951,0.992]	[4.37,4.60]*10^{-3}	[-7.32,-6.83]*10^{-5}	[-1.64,-0.21]*10^{-6}	[2.94,8.14]*10^{-7}	[-1.59,0.77]*10^{-7}	[-7.01,5.77]*10^{-8}
	III	[0.951,0.992]	[4.36,4.61]*10^{-3}	[-7.67,-6.48]*10^{-5}	[-2.67, 0.82]*10^{-6}	[-0.09,1.20]*10^{-6}	[-3.31,2.50]*10^{-7}	[-1.64,1.52]*10^{-7}
$T_{s.h2}$	I	[89.207,89.250]	[1.69,1.77]*10^{-3}	[-1.65,-1.64]*10^{-5}	[-1.35,-1.30]*10^{-7}	[4.87,4.89]*10^{-8}	[-2.23,-2.21]*10^{-9}	[-2.07,-2.03]*10^{-10}
	II	[89.207,89.250]	[1.68,1.77]*10^{-3}	[-1.70,-1.59]*10^{-5}	[-2.34,-0.30]*10^{-7}	[2.59,7.17]*10^{-8}	[-8.59,4.18]*10^{-9}	[-2.34,1.92]*10^{-9}
	III	[89.207,89.250]	[1.68,1.78]*10^{-3}	[-1.79,-1.51]*10^{-5}	[-3.83,1.18]*10^{-7}	[-0.08,1.06]*10^{-7}	[-1.80,1.36]*10^{-8}	[-5.46,5.05]*10^{-9}

results of the DMC method, and they are shown in Fig. 4. For each state variable, the upper and lower bounds of its CDF curves of DMC method are obtained as follows: for each outer-layer sampling value of the distribution parameters, a CDF curve is obtained, and the CDF curve cluster is obtained by multiple outer-layer sampling values. The solid red lines in the figure are the upper and lower bound lines of the CDF curve cluster obtained by the DMC method. The blue dashed lines, the yellow dash-dot lines and the green dotted lines are the upper and lower bounds of the CDF curves obtained by Method I, Method II and Method III.

To further compare the calculation results of Method I, Method II and Method III, the cumulants of the state variable obtained by the traditional cumulant method without considering the uncertainties of the distribution parameters (the parameters are all set as the central values of the intervals) are used as base values. The per-unit interval widths of the CIs in Table 1 are calculated, and then the average per-unit interval width each order CI are calculated and shown in Table 2. Obviously, the average per-unit interval widths of 2nd–7th order CIs of the state variables obtained by Method III are significantly larger than those obtained by Method I. And the average per-unit interval widths of CIs obtained by Method II are between those obtained by Method I and Method III. As the order increases, the interval extension of Method II and III increases rapidly.

The interval extension of the CIs will result in the interval extension of the CDF interval. In Fig. 4, it can be clearly seen from the CDF interval bounds obtained by Method III that Method III has an obvious extension problem compared to the DMC method, and it has larger errors than Method I. The CDF interval bounds obtained by Method I are very close to the results of the DMC method. In addition, although Method II can also address the interval extension problem, it is less effective than Method I. Therefore, the interval extension problem is well addressed by the proposed AA&IA-based IPEF algorithm.

B. COMPARISON OF AVERAGE ROOT MEAN SQUARE

To quantify the calculation accuracies of the proposed algorithms, the traditional average root mean square (ARMS) index is improved, and the interval ARMS indexes suitable for the IPEF algorithm are proposed, namely the lower bound index $\mathrm{ARMS_L}$ and the upper bound index $\mathrm{ARMS_U}$. The calculation steps are as follows:

1) Apply the traditional cumulant method without considering the distribution parameter uncertainties to obtain the mean μ_X and variance σ_X of the state variable X.
2) N equal division points are sampled in the interval $[(\mu_{Xi} - 3\sigma_{Xi}), (\mu_{Xi} + 3\sigma_{Xi})]$ of X, $N = 40$ in this paper.
3) The $\mathrm{ARMS_L}$ and $\mathrm{ARMS_U}$ of X can be obtained by the following formulae.

$$\mathrm{ARMS_L} = \sqrt{\sum_{i=1}^{N} (\mathrm{CDF_{IPEF.L}}(i) - \mathrm{CDF_{DMC.L}}(i))^2 / N}, \tag{48}$$

$$\mathrm{ARMS_U} = \sqrt{\sum_{i=1}^{N} (\mathrm{CDF_{IPEF.U}}(i) - \mathrm{CDF_{DMC.U}}(i))^2 / N}, \tag{49}$$

where $\mathrm{CDF_{IPEF.L}}(i)$ and $\mathrm{CDF_{IPEF.U}}(i)$ are the i-th sampling values of the lower and upper bounds of the CDF interval obtained by the proposed IPEF algorithm. Obviously, $i = 1, 2, 3 \ldots N$. $\mathrm{CDF_{DMC.L}}(i)$ and $\mathrm{CDF_{DMC.U}}(i)$ are the i-th sampling values of the lower and upper bounds of the CDF curve cluster obtained by the DMC method.

The $\mathrm{ARMS_L}$ and $\mathrm{ARMS_U}$ of the above four state variables with Methods I, II and III are calculated from Fig. 4, as shown in Table 3. Similarly, the $\mathrm{ARMS_L}$ and $\mathrm{ARMS_U}$ of all the state variables in the CCHP-CMG with Methods I, II and III are calculated, and the statistical results are shown in Table 4. For the variables of the electricity network, the $\mathrm{ARMS_L}$ and $\mathrm{ARMS_U}$ of Method I are very small: the mean values are less than 0.3%, and the maximum is only 0.609%. For the variables of the cooling/heating network, the $\mathrm{ARMS_L}$ and $\mathrm{ARMS_U}$ of Method I are still small: the mean values are less than 0.6%, and the maximum is only 0.879%. However, the $\mathrm{ARMS_L}$ and $\mathrm{ARMS_U}$ of Method III are obviously larger than those of Method I: the mean values of errors are 2.5–6%, and the maximum error is 11.087%. The $\mathrm{ARMS_L}$ and $\mathrm{ARMS_U}$ of Method II are between those of Method I and Method III. Therefore, for each type of state variables

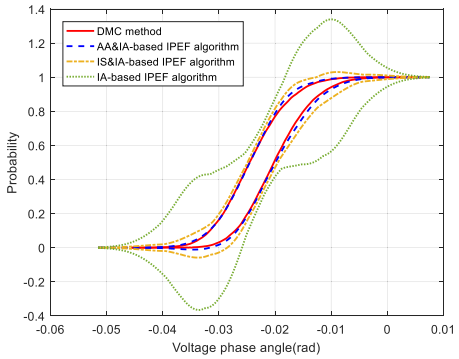

(a) Voltage phase angle at bus-2 of electricity network

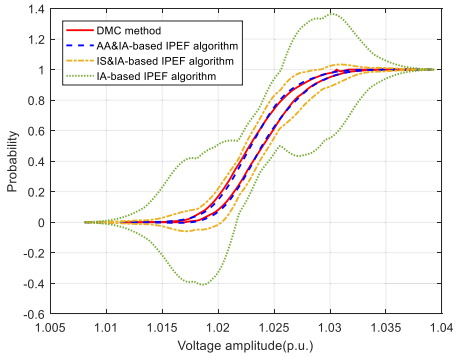

(b) Voltage amplitude at bus-2 of electricity network

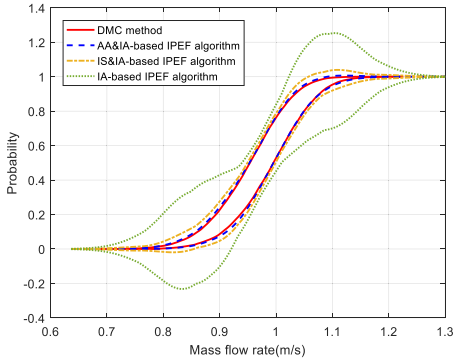

(c) Flow rate at pipe-2 of heating network

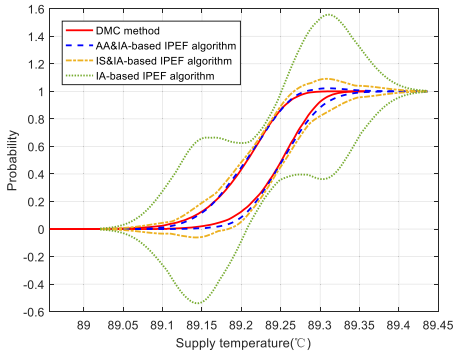

(d) Supply temperature at node-2 of heating network

FIGURE 4. CDF Intervals of several state variables.

in the IPEF calculation of the CCHP-MCG, Method I has high calculation accuracy, whereas Method III has relatively large errors. Method II is less effective than the Method I in addressing the interval extension problem. To further improve the calculation accuracy, the number of interval subdivisions must be increased, but it will greatly increase the calculation burden. Thus, Method I performs best in solving the IPEF problems.

Meanwhile, compared with the electricity network, the mean and maximum values of the error index of the cooling/heating network are obviously larger than those of the electricity network. This is because the energy flow equations of the cooling/heating network are more complicated and more nonlinear.

TABLE 2. The average per-unit values of the interval width of each order CI.

Order	1	2	3	4	5	6	7
Method I	0.062	0.039	0.003	0.038	0.005	0.010	0.021
Method II	0.062	0.043	0.068	1.541	0.940	5.792	20.673
Method III	0.062	0.051	0.167	3.781	2.320	14.328	50.815

TABLE 3. The $ARMS_L$ and $ARMS_U$ of several state variables in Figure 4.

Variable	Index	Method I	Method II	Method III
δ_2	$ARMS_L$/%	0.332	0.807	1.821
	$ARMS_U$/%	0.093	0.759	1.292
U_2	$ARMS_L$/%	0.222	1.014	5.161
	$ARMS_U$/%	0.302	0.949	4.664
m_{h1}	$ARMS_L$/%	0.274	0.410	3.940
	$ARMS_U$/%	0.329	0.661	3.685
$T_{s.h2}$	$ARMS_L$/%	0.365	0.999	5.215
	$ARMS_U$/%	0.178	0.839	5.086

TABLE 4. Statistics of the ARMS indexes of Methods I, II and III.

Variable	Method	$ARMS_L$/%		$ARMS_U$/%	
		Mean	Max	Mean	Max
δ	I	0.264	0.332	0.163	0.340
	II	0.651	1.265	0.636	1.302
	III	3.667	6.757	3.226	6.296
U	I	0.384	0.609	0.272	0.499
	II	0.637	1.109	0.452	0.950
	III	3.198	6.003	2.558	5.495
m_h	I	0.275	0.859	0.281	0.879
	II	0.696	3.661	0.981	3.554
	III	3.213	4.305	3.24	4.206
$T_{s.h}$	I	0.469	0.784	0.237	0.476
	II	1.759	4.933	1.723	4.799
	III	5.591	11.087	5.61	11.03
$T_{r.h}$	I	0.417	0.841	0.285	0.475
	II	1.126	4.014	1.151	3.785
	III	2.654	3.898	2.66	4.178
m_c	I	0.226	0.862	0.295	0.855
	II	0.583	4.473	0.598	5.196
	III	2.023	7.034	2.143	7.068
$T_{s.c}$	I	0.407	0.826	0.292	0.727
	II	1.497	5.578	1.696	6.071
	III	3.912	7.182	3.487	6.564
$T_{r.c}$	I	0.503	0.792	0.332	0.751
	II	0.531	1.647	1.111	2.890
	III	4.518	6.142	4.113	5.833

C. IPEF CALCULATION CONSIDERING THE CORRELATION AND ANALYSIS OF THE RESULTS

In this section, the correlation of node power is considered, and the calculation accuracy of the AA&IA-based IPEF algorithm considering the correlation (i.e., Method IV) is verified.

It is assumed that the correlation coefficients of different node load power and different node solar irradiances are 0.6 and 0.8, respectively. Method IV and the DMC method are applied to solve the IPEF problem. In the sampling process of the DMC method, the Nataf method is used to obtain relevant samples [14], [15]. With the results of the DMC method as a reference, the errors of the results of Method IV are calculated and shown in Table 5. It can be seen that all the mean values of the errors of Method IV are less than 0.5%, and all the maximum values are only about 1%. Therefore, the proposed AA&IA-based IPEF algorithm considering the correlation of node power has high calculation accuracy.

TABLE 5. Statistics of operation errors of Method IV.

Variable	$ARMS_L$/%		$ARMS_U$/%	
	Mean	Max	Mean	Max
δ	0.122	0.159	0.191	0.249
U	0.204	0.298	0.221	0.301
m_h	0.195	0.739	0.241	0.770
$T_{s.h}$	0.497	0.978	0.237	0.913
$T_{r.h}$	0.470	1.064	0.255	0.768
m_c	0.110	0.376	0.163	0.376
$T_{s.c}$	0.278	0.453	0.351	0.599
$T_{r.c}$	0.317	0.504	0.334	0.651

D. INFLUENCE OF DIFFERENT PV/PT PENETRATIONS ON THE ACCURACY OF IPEF CALCULATION

With the results of the DMC method as a reference, taking the voltage phase angle and amplitude at bus-2 of the electricity network, the flow rate of pipe-2, and the supply temperature at the node-2 of heating network as examples, the calculation errors of Method IV for the CCHP-CMG with different PV or PT penetrations are shown in Tables 6 and 7.

TABLE 6. Errors in cases with different PV penetrations.

PV penetration/%	Variable	$ARMS_L$	$ARMS_U$
5	δ_2	0.061	0.056
	U_2	0.081	0.079
10	δ_2	0.124	0.215
	U_2	0.157	0.211
15	δ_2	0.168	0.195
	U_2	0.192	0.229
20	δ_2	0.215	0.295
	U_2	0.228	0.317
30	δ_2	0.135	0.268
	U_2	0.141	0.275
50	δ_2	0.385	0.368
	U_2	0.364	0.357

It is observed that with the increase of PV/PT penetration, the calculation errors of Method IV also increase, but the extent of increase is relatively small. When the PV penetration reaches 50%, the calculation errors are still less than 0.4%. The reasons for the increase in errors are as follows: (1) The proposed IPEF algorithm is based on the linearized energy flow equation, so the linearization error will increase with the increase of PV or PT output fluctuation; (2) Gram-Charlier expansion causes errors in the calculation of non-normally distributed random variables of PV or PT power output, and the series expansion errors will also increase with the increase of PV or PT output fluctuation. Therefore, the higher the PV or PT penetration, the bigger the fluctuation of PV or PT output, and the greater the errors.

TABLE 7. Errors in cases with different PT penetrations.

PT penetration/%	Variable	$ARMS_L$	$ARMS_U$
5	m_{h2}	0.153	0.233
	$T_{s.h2}$	0.408	0.132
10	m_{h2}	0.374	0.432
	$T_{s.h2}$	0.542	0.181
15	m_{h2}	0.406	0.290
	$T_{s.h2}$	0.741	0.191
20	m_{h2}	0.397	0.371
	$T_{s.h2}$	0.886	0.475
25	m_{h2}	0.196	0.444
	$T_{s.h2}$	1.099	0.806
30	m_{h2}	0.266	0.568
	$T_{s.h2}$	1.163	1.032

E. INFLUENCE OF DIFFERENT CORRELATIONS ON THE ACCURACY OF IPEF CALCULATION

With the results of the DMC method as a reference, taking the same state variables in Section VI.D as examples, the calculation errors of Method IV for the CCHP-CMG considering different correlation coefficients of load power and solar irradiance are shown in Table 8. It is shown that as the correlation increases, the errors of Method IV are close. When the correlation coefficients of load power and solar irradiance both reach 0.9, the errors of voltage amplitude and angle and pipeline flow rate are less than 0.25%, and the temperature error is less than 0.5%. Combining the results in Sections VI.D and VI.E, the proposed AA&IA-based IPEF algorithm considering the correlation has high calculation accuracy, and its calculation errors remain at a small value with different correlations of node power.

TABLE 8. Comparison of errors in different correlations.

Correlation coefficient of load power	Correlation coefficient of solar irradiance	Variable	$ARMS_L$	$ARMS_U$
0.1	0.3	δ_2	0.061	0.213
		U_2	0.040	0.206
		m_{h2}	0.187	0.366
		$T_{s.h2}$	0.276	0.233
0.3	0.6	δ_2	0.061	0.231
		U_2	0.053	0.203
		m_{h2}	0.181	0.329
		$T_{s.h2}$	0.314	0.411
0.6	0.8	δ_2	0.265	0.245
		U_2	0.212	0.228
		m_{h2}	0.155	0.340
		$T_{s.h2}$	0.346	0.372
0.9	0.9	δ_2	0.124	0.165
		U_2	0.088	0.184
		m_{h2}	0.160	0.218
		$T_{s.h2}$	0.407	0.470

TABLE 9. Comparison of computation time.

Method	I	II	III	IV	DMC
Calculation time/s	2.542	108.769	2.012	2.832	349 386
Percentage/%	0.00073	0.03113	0.00058	0.00081	-

F. COMPARISON OF COMPUTATION TIME

The mean computation times of Methods I, II, III and IV and the DMC method are calculated in the cases with different PV/PT penetrations and different correlation coefficients, and the results are shown in Table 9. Compared with Method III, although the computation time of Method I is slightly increased, it can effectively address the interval extension problem in Method III and has higher calculation accuracy. Method II requires dividing the interval into subintervals and repeating the interval calculation process. Therefore, the calculation time of Method II is significantly higher than those of Methods I, III and IV, and this method is less effective in addressing the interval extension problem. The computation time of Method IV is a little higher than Method I, since it considers the correlation of node power. Moreover, the calculation time of Method IV is only 0.00081% of the calculation time of the DMC method, which has much higher calculation efficiency.

VII. CONCLUSION

In this paper, an AA&IA-based IPEF algorithm of a CCHP-CMG considering the interval uncertainties of distribution parameters of node power random variables is proposed. It uses AA to address the interval extension problem in the IA-based IPEF algorithm and has good calculation accuracy. Moreover, by constructing the correlation conversion matrixes, the correlation of node power can be considered in the proposed IPEF algorithm. The calculation results of the case study show that the proposed AA&IA-based IPEF algorithm considering the correlation can obtain accurate CDF curve fluctuation intervals of the state variables, with the results of the DMC method as a reference. The algorithm also has high calculation accuracy with different PV/PT penetrations and different correlations of node power. It has much higher calculation efficiency than the DMC method. In addition, the proposed AA&IA-based IPEF algorithm can also be applied to the traditional probability power flow calculation of power grid considering the interval uncertainties of distribution parameters of the node power random variables.

The energy flow equations related to heating/cooling networks are highly nonlinear, which will bring certain errors to the IPEF calculation results in cases with large fluctuations of uncertain variables. Therefore, dealing with the highly nonlinear characteristics of heating/cooling networks to improve the accuracy of the IPEF calculation of a CCHP-CMG is a possible direction for future research.

TABLE 10. Parameters of pipes in heating/cooling network.

Pipe	From node	To node	Length/m	Pipe	From node	To node	Length/m
1	1	43	600	26	25	26	200
2	1	2	200	27	25	27	200
3	1	3	200	28	25	28	200
4	1	4	300	29	29	25	300
5	4	5	200	30	29	30	200
6	4	6	200	31	29	31	200
7	4	7	300	32	32	29	300
8	7	8	200	33	32	33	200
9	7	9	200	34	32	34	200
10	7	10	300	35	35	32	300
11	10	11	200	36	35	36	200
12	10	12	200	37	35	37	300
13	13	10	300	38	37	38	500
14	13	14	200	39	37	39	200
15	13	15	200	40	37	40	300
16	16	13	300	41	40	41	200
17	16	17	200	42	40	42	200
18	16	18	200	43	43	40	300
19	19	16	300	44	43	44	200
20	19	20	200	45	43	45	200
21	19	21	200	46	43	46	200
22	22	19	300	47	47	22	800
23	22	23	200	48	48	35	800
24	22	24	200	49	49	1	800
25	22	25	600				

TABLE 11. Load power at nodes in the heating/cooling network.

Heating network				Cooling network			
Nodes	$\Phi_{L.h}$/MW	Nodes	$\Phi_{L.h}$/MW	Nodes	$\Phi_{L.c}$/MW	Nodes	$\Phi_{L.c}$/MW
2–3	0.1	26–28	0.1	2–3	0.3	26–28	0.3
5–6	0.1	30–31	0.1	5–6	0.3	30–31	0.3
8–9	0.1	33–34	0.1	8–9	0.3	33–34	0.3
11–12	0.1	36	0.1	11–12	0.3	36	0.3
14–15	0.1	38–39	0.1	14–15	0.3	38–39	0.3
17–18	0.1	41–42	0.3	17–18	0.3	41–42	0.3
20–21	0.1	44–46	0.3	20–21	0.3	44–46	0.3
23–24	0.1			23–24	0.3		

TABLE 12. Load power at buses in the electricity network.

Bus	P_L/MW	Q_L/MW	Bus	P_L/MW	Q_L/MW
1	0.083	0.051	50	0.322	0.200
2	0.098	0.061	51	0.044	0.027
38	0.105	0.065	52	0.062	0.038
39	0.131	0.081	77	0.316	0.190
40	0.107	0.066	78	0.096	0.060
41	0.104	0.064	79	0.094	0.058
42	0.212	0.132	80	0.306	0.190
43	0.232	0.144	81	0.332	0.206
44	0.225	0.139	82	0.462	0.283
45	0.079	0.049	83	0.167	0.081
46	0.496	0.307	84	0.461	0.286
47	0.506	0.313	85	0.281	0.186
48	0.554	0.343	86	0.363	0.242
49	0.361	0.224			

APPENDIX

The data of electricity network and heating/cooling networks are shown in Table 10 to 13. The details and other parameters of the energy flow calculation method of the network can be referred to the [23].

TABLE 13. Parameters of the branch in the electricity network.

From bus	To bus	Impedance(p.u.)	From bus	To bus	Impedance(p.u.)	From bus	To bus	Impedance(p.u.)	From bus	To bus	Impedance(p.u.)
91	37	0.0099+j0.0352	19	20	0.0042+j0.0150	23	48	0.0749+j0.5168	63	64	0.0013+j0.0046
91	87	0.0010+j0.0035	20	21	0.0023+j0.0081	24	48	0.0749+j0.5168	65	66	0.0020+j0.0072
90	37	0.0010+j0.0035	21	22	0.0023+j0.0081	25	48	0.0749+j0.5168	66	67	0.0014+j0.0049
89	87	0.0020+j0.0070	23	24	0.0023+j0.0081	26	48	0.0749+j0.5168	67	68	0.0003+j0.0010
88	37	0.0011+j0.0038	24	25	0.0017+j0.0062	27	49	0.0749+j0.5168	69	70	0.0006+j0.0022
53	37	0.0044+j0.0158	25	26	0.0012+j0.0045	28	49	0.0749+j0.5168	70	71	0.0021+j0.0076
37	3	0.0033+j0.0117	27	28	0.0012+j0.0045	29	50	0.0749+j0.5168	71	72	0.0014+j0.0049
37	6	0.0055+j0.0198	28	29	0.0031+j0.0110	30	50	0.0749+j0.5168	73	74	0.0042+j0.0150
37	7	0.0069+j0.0246	29	30	0.0012+j0.0044	31	51	0.0749+j0.5168	74	75	0.0023+j0.0081
37	10	0.0036+j0.0129	30	31	0.0012+j0.0042	32	52	0.0749+j0.5168	75	76	0.0006+j0.0020
37	11	0.0039+j0.0140	31	32	0.0014+j0.0051	33	2	0.0749+j0.5168	53	77	0.0749+j0.5168
37	14	0.0025+j0.0089	33	34	0.0044+j0.0130	34	2	0.0749+j0.5168	54	77	0.0749+j0.5168
37	15	0.0027+j0.0097	34	35	0.0036+j0.0117	35	2	0.0749+j0.5168	55	78	0.0749+j0.5168
37	18	0.0046+j0.0164	35	36	0.0035+j0.0099	36	1	0.0749+j0.5168	56	79	0.0749+j0.5168
37	19	0.0038+j0.0137	3	38	0.0749+j0.5168	87	53	0.0020+j0.0070	57	80	0.0749+j0.5168
37	22	0.0046+j0.0164	4	39	0.0749+j0.5168	87	56	0.0011+j0.0038	58	80	0.0749+j0.5168
37	23	0.0056+j0.0199	5	40	0.0749+j0.5168	87	57	0.0044+j0.0158	59	81	0.0749+j0.5168
37	26	0.0060+j0.0214	6	41	0.0749+j0.5168	87	60	0.0033+j0.0117	60	81	0.0749+j0.5168
37	27	0.0006+j0.0023	7	42	0.0749+j0.5168	87	61	0.0055+j0.0198	61	82	0.0749+j0.5168
37	32	0.0013+j0.0046	8	42	0.0749+j0.5168	87	64	0.0069+j0.0246	62	82	0.0749+j0.5168
37	33	0.0010+j0.0037	9	43	0.0749+j0.5168	87	65	0.0036+j0.0129	63	82	0.0749+j0.5168
37	36	0.0017+j0.0062	10	43	0.0749+j0.5168	87	68	0.0039+j0.0140	64	83	0.0749+j0.5168
3	4	0.0014+j0.0051	11	44	0.0749+j0.5168	87	69	0.0025+j0.0089	65	84	0.0749+j0.5168
4	5	0.0014+j0.0051	12	44	0.0749+j0.5168	87	72	0.0027+j0.0097	66	84	0.0749+j0.5168
5	6	0.0014+j0.0051	13	44	0.0749+j0.5168	87	73	0.0046+j0.0164	67	84	0.0749+j0.5168
7	8	0.0014+j0.0051	14	45	0.0749+j0.5168	87	76	0.0038+j0.0137	68	84	0.0749+j0.5168
8	9	0.0014+j0.0051	15	46	0.0749+j0.5168	53	54	0.0013+j0.0046	69	85	0.0749+j0.5168
9	10	0.0014+j0.0051	16	46	0.0749+j0.5168	54	55	0.0010+j0.0037	70	85	0.0749+j0.5168
11	12	0.0020+j0.0072	17	46	0.0749+j0.5168	55	56	0.0017+j0.0062	71	85	0.0749+j0.5168
12	13	0.0014+j0.0049	18	46	0.0749+j0.5168	57	58	0.0014+j0.0051	72	86	0.0749+j0.5168
13	14	0.0003+j0.0010	19	47	0.0749+j0.5168	58	59	0.0011+j0.0041	73	86	0.0749+j0.5168
15	16	0.0006+j0.0022	20	47	0.0749+j0.5168	59	60	0.0005+j0.0019	74	86	0.0749+j0.5168
16	17	0.0021+j0.0076	21	47	0.0749+j0.5168	61	62	0.0002+j0.0008	75	86	0.0749+j0.5168
17	18	0.0014+j0.0049	22	48	0.0749+j0.5168	62	63	0.0010+j0.0037	76	86	0.0749+j0.5168

REFERENCES

[1] P. Lopion, P. Markewitz, M. Robinius, and D. Stolten, "A review of current challenges and trends in energy systems modeling," *Renew. Sustain. Energy Rev.*, vol. 96, pp. 156–166, Nov. 2018.

[2] J. Wu, J. Yan, H. Jia, N. Hatziargyriou, N. Djilali, and H. Sun, "Integrated energy systems," *Appl. Energy*, vol. 167, pp. 155–157, 2016.

[3] Q. Hu, B. Zeng, Y. Zhang, H. Hu, and W. Liu, "Analysis of probabilistic energy flow for integrated electricity-gas energy system with P2G based on cumulant method," in *Proc. IEEE Conf. Energy Internet Energy Syst. Integr. (EI2)*, Beijing, China, Nov. 2017, pp. 1–6.

[4] H. Khorsand and A. R. Seifi, "Probabilistic energy flow for multi-carrier energy systems," *Renew. Sustain. Energy Rev.*, vol. 94, pp. 989–997, Oct. 2018.

[5] P. E. Lehner, K. B. Laskey, and D. Dubois, "An introduction to issues in higher order uncertainty," *IEEE Trans. Syst., Man, Cybern. A, Syst. Humans*, vol. 26, no. 3, pp. 289–293, May 1996.

[6] J. Weinstein and M. Yildiz, "Impact of higher-order uncertainty," *Games Econ. Behav.*, vol. 60, no. 1, pp. 200–212, Jul. 2007.

[7] P. Chen, Z. Chen, and B. Bak-Jensen, "Probabilistic load flow: A review," in *Proc. 3rd Int. Conf. Electr. Utility Deregulation Restructuring Power Technol.*, Nanjing, China, Apr. 2008, pp. 1586–1591.

[8] Z. Wang, C. Shen, F. Liu, and F. Gao, "Analytical expressions for joint distributions in probabilistic load flow," *IEEE Trans. Power Syst.*, vol. 32, no. 3, pp. 2473–2474, May 2017.

[9] D. Villanueva, J. L. Pazos, and A. Feijoo, "Probabilistic load flow including wind power generation," *IEEE Trans. Power Syst.*, vol. 26, no. 3, pp. 1659–1667, Aug. 2011.

[10] Y. Wang, N. Zhang, Q. Chen, J. Yang, C. Kang, and J. Huang, "Dependent discrete convolution based probabilistic load flow for the active distribution system," *IEEE Trans. Sustain. Energy*, vol. 8, no. 3, pp. 1000–1009, Jul. 2017.

[11] P. Zhang and S. T. Lee, "Probabilistic load flow computation using the method of combined cumulants and Gram-Charlier expansion," *IEEE Trans. Power Syst.*, vol. 19, no. 1, pp. 676–682, Feb. 2004.

[12] M. Fan, V. Vittal, G. T. Heydt, and R. Ayyanar, "Probabilistic power flow studies for transmission systems with photovoltaic generation using cumulants," *IEEE Trans. Power Syst.*, vol. 27, no. 4, pp. 2251–2261, Nov. 2012.

[13] D. Cai, J. Chen, D. Shi, X. Duan, H. Li, and M. Yao, "Enhancements to the cumulant method for probabilistic load flow studies," in *Proc. IEEE Power Energy Soc. Gen. Meeting*, San Diego, CA, USA, Jul. 2012, pp. 1–8.

[14] J. Chen, Q. Yu, Q. Li, Z. Lin, and C. Li, "Probabilistic energy flow analysis of MCE system considering various coupling units and the uncertainty of distribution generators," *IEEE Access*, vol. 7, pp. 100394–100405, Jul. 2019.

[15] L. Yang, X. Zhao, X. Hu, G. Sun, and W. Yan, "Probabilistic power and gas flow analysis for electricity-gas coupled networks considering uncertainties in pipeline parameters," in *Proc. IEEE Conf. Energy Internet Energy Syst. Integr. (EI2)*, Beijing, China, Nov. 2017, pp. 1–6.

[16] S. Chen, Z. Wei, G. Sun, K. W. Cheung, and Y. Sun, "Multi-linear probabilistic energy flow analysis of integrated electrical and natural-gas systems," *IEEE Trans. Power Syst.*, vol. 32, no. 3, pp. 1970–1979, May 2017.

[17] X. Hu, X. Zhao, and X. Feng, "Probabilistic-interval energy flow analysis of regional integrated electricity and gas system considering multiple uncertainties and correlations," *IEEE Access*, vol. 7, pp. 178209–178223, Dec. 2019.

[18] X. Guo, R. Gong, H. Bao, and Q. Wang, "Hybrid stochastic and interval power flow considering uncertain wind power and photovoltaic power," *IEEE Access*, vol. 7, pp. 85090–85097, Jun. 2019.

[19] M. Lubin, Y. Dvorkin, and S. Backhaus, "A robust approach to chance constrained optimal power flow with renewable generation," *IEEE Trans. Power Syst.*, vol. 31, no. 5, pp. 3840–3849, Sep. 2016.

[20] J. Zhou, W. Liu, X. Chen, M. Sun, C. Mei, S. He, H. Gao, and J. Liu, "A distributionally robust chance constrained planning method for integrated energy systems," in *Proc. IEEE PES Asia–Pacific Power Energy Eng. Conf. (APPEEC)*, Macao, China, Dec. 2019, pp. 1–5.
[21] Z. Wang, Q. Bian, H. Xin, and D. Gan, "A distributionally robust co-ordinated reserve scheduling model considering CVaR-based wind power reserve requirements," *IEEE Trans. Sustain. Energy*, vol. 7, no. 2, pp. 625–636, Apr. 2016.
[22] H. Wu, P. Dong, and M. Liu, "Random fuzzy power flow of distribution network with uncertain wind turbine, PV generation, and load based on random fuzzy theory," *IET Renew. Power Gener.*, vol. 12, no. 10, pp. 1180–1188, Jul. 2018.
[23] X. Liu, J. Wu, N. Jenkins, and A. Bagdanavicius, "Combined analysis of electricity and heat networks," *Appl. Energy*, vol. 162, pp. 1238–1250, Jan. 2016.
[24] S. Karaki, R. Chedid, and R. Ramadan, "Probabilistic performance assessment of autonomous solar-wind energy conversion systems," *IET Renew. Power Gener.*, vol. 14, no. 3, pp. 766–772, 1999.
[25] R. E. Moore, R. B. Kearfott, and M. J. Cloud, *Introduction to Interval Analysis*. Philadelphia, PA, USA: Siam, 2009.
[26] L. H. de Figueiredo and J. Stolfi, "Affine arithmetic: Concepts and applications," *Numer. Algorithms*, vol. 37, nos. 1–4, pp. 147–158, Dec. 2004.
[27] G. Alefeld and G. Mayer, "The Cholesky method for interval data," *Linear Algebra Appl.*, vol. 194, pp. 161–182, Nov. 1993.
[28] G. Alefeld and G. Mayer, "New criteria for the feasibility of the Cholesky method with interval data," *SIAM J. Matrix Anal. Appl.*, vol. 30, no. 4, pp. 1392–1405, Jan. 2009.
[29] J. Garloff, "Pivot tightening for the interval Cholesky method," *PAMM*, vol. 10, no. 1, pp. 549–550, Dec. 2010.
[30] Z. Liao, S. Chen, and C. Lin, "Voltage state assessment of distribution network with distributed photovoltaic correlation based on improved nataf transformation and cumulant method," in *Proc. Int. Conf. Power Syst. Technol. (POWERCON)*, Guangzhou, China, Nov. 2018, pp. 4208–4214.
[31] S. M. Rump, "INTLAB—Interval laboratory," in *Developments in Reliable Computing*, 1st ed. Dordrecht, The Netherlands: Springer, 1999, pp. 77–104.

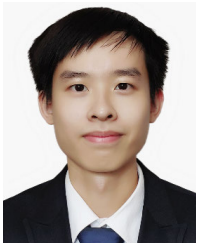

YUQUAN XIE received the B.S. degree in electrical engineering from the South China University of Technology, in 2019, where he is currently pursuing the M.S. degree with the School of Electric Power Engineering. His research interests include the uncertainty analysis and optimization of integrated energy systems.

SHUNJIANG LIN (Member, IEEE) received the B.S. degree in electrical engineering from the South China University of Technology, in 2003, and the Ph.D. degree in electrical engineering from Hunan University, in 2008. He is currently an Associate Professor with the School of Electric Power Engineering, South China University of Technology. His research interests include the uncertainty analysis and optimization of integrated energy systems.

WEIKUN LIANG received the B.S. degree in electrical engineering from the South China University of Technology, where he is currently pursuing the M.S. degree with the School of Electric Power Engineering. His research interests include the uncertainty analysis and optimization of integrated energy systems.

YUERONG YANG received the B.S. degree in electrical engineering from the South China University of Technology, in 2019, where he is currently pursuing the M.S. degree with the School of Electric Power Engineering. His research interests include power system optimization, operation, and control.

ZHIQIANG TANG received the B.S. degree in electrical engineering from Zhengzhou University, in 2018. He is currently pursuing the M.S. degree with the School of Electric Power Engineering, South China University of Technology. His research interests include the uncertainty analysis and optimization of integrated energy systems.

YUNONG SONG received the B.S. degree in electrical engineering from the South China University of Technology, in 2016, where he is currently pursuing the M.S. degree with the School of Electric Power Engineering. His research interests include power system optimization, operation, and control.

MINGBO LIU (Member, IEEE) received the B.S. degree from the Huazhong University of Science and Technology, in 1985, the M.S. degree from the Harbin Institute of Technology, in 1988, and the Ph.D. degree from Tsinghua University, in 1992. He is currently a Professor with the South China University of Technology. He has authored or coauthored four monographs, two standards, and more than 280 articles. His research interests include energy management and operation control of power systems.